Published in final edited form as:
Methods. 2014 March 15; 66(2): 131–138. doi:10.1016/j.ymeth.2013.06.021.

Estimating the distance separating fluorescent protein FRET pairs

Steven S. Vogel[a], **B. Wieb van der Meer**[b], and **Paul S. Blank**[c]

Steven S. Vogel: stevevog@mail.nih.gov

[a]Laboratory of Molecular Physiology, National Institute on Alcohol Abuse and Alcoholism, National Institutes of Health, 5625 Fishers Lane, Room TS-06F: MSC 9411, Bethesda, MD 20892-9413, USA

[b]Department of Physics and Astronomy, Western Kentucky University, 1906 College Heights Blvd. #11077, Bowling Green, KY 42101-1077, USA

[c]Program in Physical Biology, Eunice Kennedy Shriver National Institute of Child Health and Human Development, National Institutes of Health, 10 Center Dr, Room 10D14: MSC 1855, Bethesda, MD 20892-1855, USA

Abstract

Förster resonance energy transfer (FRET) describes a physical phenomenon widely applied in biomedical research to estimate separations between biological molecules. Routinely, genetic engineering is used to incorporate spectral variants of the green fluorescent protein (GFPs), into cellular expressed proteins. The transfer efficiency or rate of energy transfer between donor and acceptor FPs is then assayed. As appreciable FRET occurs only when donors and acceptors are in close proximity (1–10 nm), the presence of FRET may indicate that the engineered proteins associate as interacting species. For a homogeneous population of FRET pairs the separations between FRET donors and acceptors can be estimated from a measured FRET efficiency if it is assumed that donors and acceptors are randomly oriented and rotate extensively during their excited state (dynamic regime). Unlike typical organic fluorophores, the rotational correlation-times of FPs are typically much longer than their fluorescence lifetime; accordingly FPs are virtually static during their excited state. Thus, estimating separations between FP FRET pairs is problematic. To overcome this obstacle, we present here a simple method for estimating separations between FPs using the experimentally measured average FRET efficiency. This approach assumes that donor and acceptor fluorophores are randomly oriented, but do not rotate during their excited state (static regime). This approach utilizes a Monte-Carlo simulation generated look-up table that allows one to estimate the separation, normalized to the Förster distance, from the average FRET efficiency. Assuming a dynamic regime overestimates the separation significantly (by 10% near 0.5 and 30% near 0.75 efficiencies) compared to assuming a static regime, which is more appropriate for estimates of separations between FPs.

Keywords

GFP; Kappa squared

Correspondence to: Steven S. Vogel, stevevog@mail.nih.gov.

1. Introduction

The discovery and optimization of genetically encoded fluorophores [1,2], such as green fluorescent protein (GFP) and its derivatives (FPs), has stimulated interest in using microscopy to identify and measure protein–protein interactions within living cells [3,4]. Förster resonance energy transfer (FRET) describes a physical phenomenon in which energy is transferred from a donor fluorophore in its excited state to a near-by acceptor fluorophore in its ground state [3–8]. FRET can only occur between a pair of molecules that utilize approximately the same amount of energy to transition between their ground and excited states. Specifically, the energy liberated when an excited donor transitions to its ground state must be equivalent to the energy required to excite an acceptor. The suitability for two fluorescent molecules to transfer energy using FRET is proportional to the overlap of the donor emission and acceptor absorption spectra or overlap integral, *J*. For a pair of fluorophores with non-zero *J*, the FRET transfer rate constant, k_T, has an inverse sixth power dependence on the distance between donor and acceptor fluorophores (R_{DA}).

$$k_T = \frac{1}{\tau_{0D}} \left(\frac{R_0}{R_{DA}} \right)^6 \quad (1)$$

where τ_{0D} is the fluorescence lifetime of the donor, and R_0 is the Förster distance, the separation at which 50% of the donor excitation events result in energy transfer to the acceptor for a particular donor-acceptor pair. The value of R_0 is given by:

$$R_0 = \sqrt[6]{\frac{9\ln(10)}{128\pi^5 N'} \frac{\kappa^2 Q_D J}{n^4}} = 0.02108 \sqrt[6]{\kappa^2 n^{-4} Q_D J} \text{nm} \quad (2)$$

where N' is Avogadro's number per mmole, 6.022×10^{20}, n the refractive index of the nearby medium [9], κ^2 the orientation factor for dipole–dipole coupling, which equals 2/3 in the dynamic isotropic limit, R_0 is R_0 when kappa-squared is 2/3, Q_D the fluorescence quantum yield of the donor in the absence of the acceptor, and the numerical factor 0.02108 applying when *J* is defined in units of nm^4 cm^2/mmole.

Energy transfer efficiency, *E*, is defined by the ratio of the transfer rate constant to the total donor deactivation rate:

$$E = \frac{k_T}{\frac{1}{\tau_{0D}} + k_T} \quad (3)$$

Substitution from Eq. (1) for k_T reveals that *E* does not depend on the donor lifetime, only on R_0 and R_{DA}:

$$E = \frac{(R_0/R_{DA})^6}{1 + (R_0/R_{DA})^6} \quad (4)$$

Using Eq. (4), the FRET efficiency can be used to estimate the distance separating fluorescently labeled sites (R_{DA}) within and between biomolecules [10,11]. In most FRET experiments the average FRET efficiency, $\langle E \rangle$, is measured for a population of potential donors and acceptors, not the FRET efficiency, *E*, for an individual pair. Accordingly, to estimate distances from an experimentally measured average FRET efficiency it is either

assumed that all donors in the population are paired with acceptors that have approximately the same FRET efficiency, or corrections are required to account for those donors that are not paired with an acceptor or have significantly different FRET efficiencies [11,12].

In addition to separation, the FRET transfer rate is also dependent on the angular position of the acceptor relative to the donor's emission dipole vector (θ), and on the orientation of the acceptors absorption dipole vector relative to the electric field of the donor at the acceptors location (ω) [13–15]. These two angles define κ^2, the orientation factor for the required dipole–dipole coupling.

$$\kappa^2=(1+3\cos^2\theta)\cos^2\omega \quad (5)$$

Because $\cos^2\theta$ and $\cos^2\omega$ can have values ranging from 0 to 1, κ^2 can have values ranging from 0 to 4. The physical basis of κ^2 is depicted in Fig. 1A. Based on Eqs. (1), (2), and (4) it is clear that if κ^2 is zero, FRET cannot occur, while if κ^2 is 4, the maximal rate and FRET efficiency can be achieved for any specific separation. In biological FRET experiments the actual values for θ, ω, and therefore κ^2 are not known. For free donors and acceptors in solution, and often for fluorophores coupled to biological molecules via a flexible linker, it is assumed that θ and ω have random orientations (*isotropic*). With this 'isotropic' assumption, the probability distribution of κ^2 values will range from 0 to 4, with a mode value of 0 and an average value of 2/3 (Fig. 1B). In most FRET experiments, and when calculating the Förster distance (R_0) for a specific donor-acceptor pair, κ^2 is assumed to have a value of 2/3 [15–18]. The use of 2/3, the average value for κ^2 in an isotropic distribution, in FRET calculations is predicated on the assumptions that (1) θ and ω have random orientations (from an isotropic distribution of orientations), and (2) that during the donors excited state lifetime the values of θ and ω change rapidly and independently as a result of rapid molecular rotation [18]. For non-tethered, or loosely tethered small organic fluorophores that can rotate rapidly relative to their fluorescence lifetimes it is reasonable to assume that θ and ω will assume many different random orientations during the excited state lifetime of the donor, thus the average value of the κ^2 probability distribution, 2/3, can be used in calculations. With these assumed conditions, formally called *dynamic isotropic*, donor-acceptor separation can be calculated from a measured average FRET efficiency and the Förster distance for the specific donor-acceptor pair.

$$R_{DA}=\sqrt[6]{\frac{\overline{R}_0^6}{\langle E\rangle}-\overline{R}_0^6}=\overline{R}_0\cdot\sqrt[6]{\frac{1}{\langle E\rangle}-1} \quad (6)$$

Eq. (6) can be rewritten as:

$$R_{DA}=\overline{R}_0\cdot\Phi \quad (7)$$

where Φ is:

$$\Phi=\frac{R_{DA}}{\overline{R}_0}=\sqrt[6]{\frac{1}{\langle E\rangle}-1} \quad (8)$$

Φ is the separation normalized to the Förster distance and can be thought of as the fractional dependence of R_{DA} on $\langle E\rangle$. Unfortunately, Eqs. (6 and 8) cannot be used for large fluorophores, such as GFP, because the κ^2 value of 2/3, inherent in the R_0 value of Eqs. (6)

and (8), is not appropriate for a random isotropic population of FRET donors and acceptors that rotate slowly relative to the excited state lifetime of the donor [14,15,18,19]. In fact, under these conditions, formally called the *static random isotropic orientational regime*, there is no single value for κ^2 that is appropriate for all separations [15,16]. Nonetheless, Eq. (7) does describe the correspondence between $\langle E \rangle$ and R_{DA} in the *static random isotropic orientational regime*, but there is no simple equation, such as Eq. (8), for calculating the value Φ as a function of $\langle E \rangle$. Here we use Monte Carlo simulations to generate a look-up table applicable to FPs, that can be used in conjunction with Eq. (7) to estimate distances between FP donors and acceptors based on experimentally determined average FRET efficiencies.

2. Methods

2.1. Monte Carlo simulations

Monte Carlo simulations were performed in Igor Pro (ver6.22) to generate populations of FRET efficiencies in the static random isotropic orientational regime. Each simulation was based on generating 1,000,000 random replicate E values for a given Φ value. Two hundred and fifty Φ values were generated between a starting value of 0.01 and a final value of 2.5 in 0.01 increments. For each replicate the following equation was used to calculate a single FRET efficiency:

$$E_{static} = \frac{\kappa^2 \cdot \frac{3}{2} \cdot \left(\frac{1}{\Phi}\right)^6}{\kappa^2 \cdot \frac{3}{2} \cdot \left(\frac{1}{\Phi}\right)^6 + 1} \quad (9)$$

where κ^2 was stochastically generated for each replicate to simulate FRET in the isotropic static regime. A distribution of 1,000,000 κ^2 values was generated from random values for the angles θ and ω, generated as previously described [18]. In brief, a uniform distribution of numbers ranging from 0 to 1 was generated using the Igor Pro ***enoise*** command. Next, the inverse cosine of these values was calculated to generate a population of angles expected for an isotropic distribution. These values of θ and ω were used in Eq. (5) to generate the population of κ^2 values, and these in turn were used in Eq. (9) to calculate FRET efficiencies in the static regime.

The average FRET efficiency, $\langle E \rangle$, standard deviation, SD, skewness, and kurtosis of Monte Carlo simulation generated FRET efficiency populations were calculated using the Igor Pro ***wavestats*** command, using the following equations:

$$\langle E \rangle = \frac{\sum_{i=0}^{i=999,999} E_i}{1,000,000} \quad (10)$$

$$SD = \sqrt{\frac{1}{999,999} \sum \left(E - \langle E \rangle\right)^2} \quad (11)$$

$$Skewness = \frac{1}{1,000,000} \sum_{i=0}^{i=999,999} \left[\frac{E - \langle E \rangle}{SD}\right]^3 \quad (12)$$

$$Kurtosis = \frac{1}{1,000,000} \sum_{i=0}^{i=999,999} \left[\frac{E - \langle E \rangle}{SD} \right]^4 - 3 \quad (13)$$

3. Results

Monte Carlo simulations were used to model the distribution of FRET efficiencies in 250 populations each having progressively larger separations. The Förster distance was set to 1 in these simulations and the separations varied, in Förster distance units, from 0.01 to 2.5 in 0.01 increments for each population. When the Förster distance is normalized to a value 1, the distance, R_{DA}, is equivalent to Φ, the Förster distance normalized dependence of R_{DA} on $\langle E \rangle$. Each individual simulation population consisted of 1 million FRET pairs each with the same separation but with random isotropic values for θ and ω. Probability density histograms, $p(E)$, of three of these populations are plotted in Fig. 2. These correspond to *static isotropic* populations with Φ values of 0.66 (panel A), 0.89 (B), and 1.14 (C), and average FRET efficiencies $\langle E \rangle$, of 0.75, 0.50, and 0.25, respectively. These FRET efficiency probability distributions are broad, and strikingly non-Gaussian. In each case the mean of the distribution is dramatically different from the population mode and median. This can be quantified by examining the *skewness* (symmetry around the mean) and *kurtosis* (peakedness) of these distributions; a Gaussian distribution has zero skewness and kurtosis.

We have previously described an analytical solution for the probability density $p(E)$ of FRET efficiencies in *static isotropic regime* populations [18]. These distributions have 3 phases, the first describes the probability of having a FRET efficiency, E, falling between zero and $F/(1 + F)$, is defined by Eq. (14):

$$P(E) = \frac{1}{2(1-E)\sqrt{3E \cdot F(1-E)}} \cdot \ln(2+\sqrt{3}) \text{ for } 0 \le E \le F/(1+F) \quad (14)$$

where F, is defined as:

$$F = \frac{3}{2}\left(\frac{1}{\Phi}\right)^6 \quad (15)$$

Note, for this first phase the most probable FRET efficiency is zero. The second phase, describes the probability of having FRET efficiencies between $F/(1 + F)$ and $4F/(1 + 4F)$ and is described by Eq. (16):

$$P(E) = \frac{1}{2(1-E)\sqrt{3E \cdot F(1-E)}} \cdot \ln\left(\frac{2+\sqrt{3}}{\sqrt{\frac{E}{F(1-E)}} + \sqrt{\frac{E}{F(1-E)} - 1}}\right) \text{ for } F/(1+F) \le E \le 4F/(1+4F) \quad (16)$$

This second phase has a peak at $F/(1 + F)$ and decreases to its lowest probability at $4F/(1 + 4F)$. The third phase has a value of zero for all FRET efficiencies greater than $4F/(1 + 4F)$.

For each of the 250 simulated populations the mean FRET efficiency, the standard deviation of the mean FRET efficiency, the population skewness, and kurtosis was calculated and is plotted in Fig. 3. In panel 3A the dependence of $\langle E \rangle$ on Φ is plotted for the *static isotropic regime* (RED curve) and for comparison the dependence of E on Φ using Eq. (4) with a R_0 value of 1 is plotted for the *dynamic isotropic regime* (dashed BLUE curve). Note that in the *dynamic isotropic regime* the FRET efficiency is 50% when Φ equals 1. This is not true in

the *static isotropic regime*, where a FRET efficiency of 50% is observed when Φ equals ~0.89 (see Fig. 2B). The *dynamic* and *static* isotropic curves are nearly identical when Φ has a value greater than 1.4. Fig. 3B depict how the standard deviations of the FRET efficiency distributions in the *static isotropic regime* change as a function of Φ. When Φ equals 0.51 the standard deviation of the population is greater than 25% of the average FRET efficiency. As Φ increases, the fractional deviation observed in these populations asymptotical approaches the mean FRET efficiency. It is clear that most of these distributions are quite broad. Fig. 3C and D depict the skewness and kurtosis of these FRET efficiency distributions. These values are generally different from zero, the value expected for a Gaussian distribution.

The objective of this study is to devise a simple method to estimate the distance between a FRET pair in the static isotropic regime, based on experimentally determined average FRET efficiency values. Because of the complex and non-Gaussian shapes of the probability density histograms for FRET pairs in the static isotropic regime, solving for a simple analytical equation that accurately describes how R_{DA} changes as a function of $\langle E \rangle$ in the static isotropic regime is challenging. Accordingly, we decided upon a simpler (albeit less elegant) strategy based on generating a lookup table of sufficient precision, that equates experimentally-measured average FRET efficiency values to specific and unique values of Φ. Multiplying Φ value derived from this table by the Förster distance (R_0) of the specific FRET pair used in an experiment will then yield an estimated separation (see Eq. (7)). Sets of 250 Monte Carlo simulations, as described above for Fig. 3, were repeated in triplicate. The mean $\langle E \rangle$ value of the three replicates for each of the 250 different Φ values is presented in Table 1 with the unique Φ values used to generate these values in the Monte Carlo simulations. The average FRET efficiencies ranged from 0.999 to 0.004, with FRET efficiency increments of ~0.012 or lower. An alternative to Monte Carlo simulation is a mixed analytical-numerical approach based on simplifying the $E^*p(E)$ integral from $E = 0$ to $E = 4F/(1 + 4F)$ over the two non-zero phases of $p(E)$ given in Eqs. (14) and (16), resulting in the following expression:

$$\langle E \rangle = 1 - \frac{\sqrt{2}}{3}\Phi^3 \int_1^2 \frac{\tan^{-1}\left(\sqrt{\frac{3}{2}} \cdot x \cdot \Phi^{-3}\right)}{\sqrt{x^2 - 1}} dx \quad (17)$$

where $x = \sqrt{\kappa^2}$. For $\Phi \gg 1$, $\langle E \rangle_{\Phi \gg 1} = \Phi^{-6}$, and for $\Phi \ll 1$, $\langle E \rangle_{\Phi << 1} = 1 - \frac{\pi \cdot \ln(2+\sqrt{3})}{3\sqrt{2}}\Phi^3$. Outside of these limiting regions, the integral in Eq. (17) must be done numerically. For Φ values of 0.3, 1.0, and 2.0, numerical integration was used to validate the Monte Carlo algorithm and confirm the values in Table 1 (data not shown). For our purposes, the simplicity of the Monte Carlo algorithm was preferable to numerical integration of Eq. (17).

The data from Table 1 is plotted in Fig. 4 to illustrate the dependence of normalized separation (Φ) on the average FRET efficiency, $\langle E \rangle$, under isotropic static conditions. The dependence of Φ on $\langle E \rangle$ is quasi-linear between average FRET efficiency values 0.17 and 0.90, but is highly non-linear at extreme values of $\langle E \rangle$ (RED tinted regions of Fig. 4 and Table 1). The RED tinted regions of Table 1 should not be used for estimating separation from experimental FRET efficiencies because in these regions small errors in $\langle E \rangle$ result in large errors in Φ. A table listing Förster distances (R_0) for 19 popular fluorescent protein FRET pairs is presented Table 2.

To illustrate how Tables 1 and 2 can be used to estimate distances from experimentally determined average FRET efficiencies between fluorescent protein donors and acceptors we

applied this strategy to estimate the distance between mCerulean and mVenus in five commonly used FRET reference standards: C5V, C17V, C32V, C40V, and C50V [20,21]. Each of these constructs has a Cerulean donor fluorophore and a Venus acceptor fluorophore connected by a variable length amino acid linkers consisting of 5, 17, 32, 40, and 50, amino acids respectively. As expected, the average FRET efficiency, $\langle E \rangle$, measured for these constructs decreases as the amino acid linker length increases (see Table 3). To estimate separation in the isotropic static regime average FRET efficiency values were first transformed into Φ values using Table 1. Next these corresponding Φ values were multiplied by 5.3, the Förster distance (R_0) for the mCerulean–mVenus FRET pair (from Table 2) in nanometers. This calculation yields the estimated separations (R_{DA} Static, Table 3, RED font) between Cerulean and Venus in these constructs under the assumption that the static isotropic condition is applicable. Note that for the C50V construct the measured average FRET efficiency was 0.13, a value that falls in the non-linear portion of Table 1. Thus, the predicted separation between mCerulean and mVenus of 7.1 nm for this construct might be imprecise. For comparison, Eq. (6) was used to calculate the estimated separation distance (R_{DA} *Dynamic*, Table 3, ORANGE font) for these constructs with the assumption of dynamic isotropic conditions, i.e. $\kappa^2 = 2/3$. Furthermore, errors in the published values of R_0 will influence the accuracy of separation determinations.

The approach outlined above for estimating separation under static isotropic conditions should be applied to multiple replicates of average FRET efficiency measurements, rather than to the average of such measurements, so that errors in $\langle E \rangle$ measurements or in extrapolation using Table 1 can be accounted for in terms of the error in estimated separation.

4. Discussion

Monte Carlo simulations were used to generate a look-up table equating the average measured FRET efficiency, $\langle E \rangle$, to the Förster distance normalized separation, Φ, for resonance energy transfer occurring in the *static random isotropic orientational regime* (Table 1). FRET efficiency derived Φ values can be multiplied by the Förster distance for the specific FRET pair used (see Table 2) to estimate the distance between a donor transferring energy to an acceptor. We have used a set of FRET constructs with 5 different amino-acid linker lengths connecting mCerulean to mVenus to demonstrate how distances can be estimated from FRET measurements and compared this approach with the widely used approach for estimating distance by assuming that κ^2 has a value of $\frac{2}{3}$ (applicable only to the *dynamic random isotropic orientational regime*). For all five constructs the estimated distances using the approach outlined here was shorter than estimates assuming an *isotropic dynamic* regime (see Table 3). Differences between the estimated distances calculated using these two methods were more pronounced for samples with higher FRET efficiencies.

The validity of this method for estimating distances relies on certain assumptions: (1) Energy transfer occurs between a single donor excited state and a single ground-state acceptor, (2) There is a discrete separation between the donor and the acceptor, (3). This distance represents a homogeneous population of separations, (4) The orientation of the donor's emission dipole and the acceptor's absorption dipole is random (*isotropic*), (5) The separation and relative orientation of the donor and acceptor dipoles do not change during the excited state of the donor (*static*), (6) Donor and acceptor chromophores do not participate in blinking, bleaching, or any other photo-physical process that may modulate their ability to act as a FRET donor or acceptor. The more standard method of estimating distances by using Eq. (6) and assuming that $\kappa^2 = \frac{2}{3}$ relies on all of the same assumptions listed above except for assumption 5. To use Eq. (6) it must be assumed that during the donors excited state the distance between the donor and acceptor does not change, but the

donor and acceptor orientations relative to each other change rapidly (*dynamic*) and randomly (*isotropic* relationship is maintained). Because fluorescent proteins rotate much slower relative to their excited state lifetimes, it is clear that the *static* assumption listed above better represents the conditions under which FRET between fluorescent proteins occurs than does the *dynamic* orientational assumption. Each of the other assumptions outlined here must be thoughtfully considered before applying this approach to a specific biological FRET measurement. For example, an enzyme often exists in two different states, inactive and active. When such a protein is engineered with a FRET donor and acceptor, two distinct donor and acceptor separations might be observed, corresponding to the active and inactive states. In a cell there can be multiple copies of this engineered enzyme and therefore an ensemble FRET measurement from a cell, or even a sub-cellular compartment, might represent a heterogeneous population (see assumption 3 above) comprised, in this example, of a mixture of two discrete separations. To accurately estimate the separation of each state, and the relative abundance of these states, some strategy must be developed (such as the use of mutants that are always active or always inactive) in which the average FRET efficiency of each state can be measured from a homogenous population. The method described here can then be used to estimate the separation from $\langle E \rangle$ for each of these two states. Furthermore, once these average FRET efficiencies have been determined, linear algebra can be used to approximate the relative abundance of these two states in a heterogeneous population.

The dimensions of fluorescent proteins, roughly cylindrical with a diameter of ∼2 nm and a length of ∼4 nm [22,23], should be considered when estimating separation from FRET data. It is unlikely that donors and acceptors of this size and shape can assume a truly random population of dipole orientations, the isotropic assumption, if these molecules are on average closer than 4 nm from each other. At these close distances steric hindrance between individual fluorescent protein surfaces are likely to limit the possible orientations of the two dipoles involved in FRET. For example, using the mCerulean-mVenus FRET pair, with a R_0 value of 5.3 nm (Table 2), experimentally determined average FRET efficiencies higher than 0.65 would at first glance indicate a separation of less than 4 nm assuming static isotropic conditions. But as just mentioned, at these distances isotropic distributions are unlikely, so the validity of this estimation must be questioned. Such high average FRET efficiency values could also indicate the presence of multiple FRET acceptors [4,24], or non-random dipole orientations; the assumptions required for estimating distance under static isotropic conditions outlined here would not be warranted.

In biological experiments, less than ideal experimental conditions and reagents might undermine the application of this approach. For example, some fluorescent proteins are thought to have multiple excited states [25–27], as well as flickering or blinking activity [28–30]. Extended imaging might also result in partial bleaching of donors and acceptors at different rates. Differential rates of fluorescent protein biosynthesis and chromophore maturation might yield similar aberrant results [31]. Furthermore, with free donors and acceptors (intermolecular FRET) it is unlikely that every donor in the population will be paired with one and only one acceptor. Even when donors are coupled to an acceptor at a 1:1 ratio in a single construct, as is often the case for biosensors, the linkers used might result in a heterogeneous distribution of separations [18], as well as correlated donor and acceptor dipole orientations [32]. Corrections for many of the departures from the assumptions used in our method have been published [11,12], and potentially can be adapted for use with Table 1 to yield more accurate estimates of FRET distances in the *static* regime. We emphasize that the approach described yields only an estimate of the distance between *static* donors and acceptors. However, our approach yields more accurate estimates of separation for FRET between fluorescent proteins from an isotropic population than calculations based on dynamic conditions.

5. Note added in proof

It has recently come to our attention that R.E. Dale has described an approximation for estimating the value of $<\kappa^2>$ in the isotropic static regime (Acta Physica Polonica Vol. A54, pg 743-56,1978.). Using the 'Dale approximation', $\langle\kappa^2\rangle \approx \frac{2}{3}(1-\langle E\rangle)$, an alternative method for estimating separation in the static isotropic regime as a function of <E> can be readily formulated. Using this approach we derive, $R_{DA} \approx \overline{R}_0 \cdot \sqrt[6]{(1-\langle E\rangle)^2/\langle E\rangle}$. This equation yields distance values in excellent agreement with the values presented in Table I with deviation typically ≤ 1%.

Acknowledgments

This work was funded by intramural programs of the National Institutes of Health, National Institute on Alcohol Abuse and Alcoholism, and the Eunice Kennedy Shriver National Institute of Child Health and Human Development Bethesda, MD 20892, USA.

References

1. Chalfie M, Tu Y, Euskirchen G, Ward WW, Prasher DC. Science. 1994; 263:802–805. [PubMed: 8303295]
2. Heim R, Prasher DC, Tsien RY. Proc Natl Acad Sci USA. 1994; 91:12501–12504. [PubMed: 7809066]
3. Clegg, RM. FRET and FLIM Techniques. Gadella, TWJ., editor. Elsevier; Amsterdam: 2009. p. 1-57.
4. Vogel SS, Thaler C, Koushik SV. Sci STKE. 2006; 2006:re2. [PubMed: 16622184]
5. Jares-Erijman EA, Jovin TM. Curr Opin Chem Biol. 2006; 10:409–416. [PubMed: 16949332]
6. Sekar RB, Periasamy A. J Cell Biol. 2003; 160:629–633. [PubMed: 12615908]
7. Piston DW, Kremers GJ. Trends Biochem Sci. 2007; 32:407–414. [PubMed: 17764955]
8. Förster, T. Fluoreszenz Organischer Verbindungen. Vandenhoeck & Ruprecht; Göttingen: 1951.
9. Knox RS, van Amerongen H. J Phys Chem B. 2002; 106:5289–5293.
10. Stryer L, Haugland RP. Proc Natl Acad Sci USA. 1967; 58:719–726. [PubMed: 5233469]
11. Hoppe A, Christensen K, Swanson JA. Biophys J. 2002; 83:3652–3664. [PubMed: 12496132]
12. Wlodarczyk J, Woehler A, Kobe F, Ponimaskin E, Zeug A, Neher E. Biophys J. 2008; 94:986–1000. [PubMed: 17921223]
13. Dale RE, Eisinger J. Proc Natl Acad Sci USA. 1976; 73:271–273. [PubMed: 1061130]
14. Dale RE, Eisinger J, Blumberg WE. Biophys J. 1979; 26:161–193. [PubMed: 262414]
15. van der Meer BW. J Biotechnol. 2002; 82:181–196. [PubMed: 11999689]
16. Steinberg, IZ.; Haas, E.; Katchalski-Katzir, E. Time-Resolved Fluorescence Spectroscopy in Biochemistry and Biology. Cundall, RB.; Dale, RE., editors. Plenum Press; New York: 1983. p. 411-450.
17. Lakowicz, JR. Principles of Fluorescence Spectroscopy. third. Springer; New York: 2006.
18. Vogel SS, Nguyen TA, van der Meer BW, Blank PS. PLoS One. 2012; 7:e49593. [PubMed: 23152925]
19. Hunt J, Keeble AH, Dale RE, Corbett MK, Beavil RL, Levitt J, Swann MJ, Suhling K, Ameer-Beg S, Sutton BJ, Beavil AJ. J Biol Chem. 2012
20. Chen H, Puhl HL 3rd, Koushik SV, Vogel SS, Ikeda SR. Biophys J. 2006; 91:L39–41. [PubMed: 16815904]
21. Koushik SV, Chen H, Thaler C, Puhl HL 3rd, Vogel SS. Biophys J. 2006; 91:L99–L101. [PubMed: 17040988]
22. Rekas A, Alattia JR, Nagai T, Miyawaki A, Ikura M. J Biol Chem. 2002; 277:50573–50578. [PubMed: 12370172]

23. Malo GD, Pouwels LJ, Wang M, Weichsel A, Montfort WR, Rizzo MA, Piston DW, Wachter RM. Biochemistry. 2007; 46:9865–9873. [PubMed: 17685554]
24. Koushik SV, Blank PS, Vogel SS. PLoS One. 2009; 4:e8031. [PubMed: 19946626]
25. Heikal AA, Hess ST, Baird GS, Tsien RY, Webb WW. Proc Natl Acad Sci USA. 2000; 97:11996–12001. [PubMed: 11050231]
26. Heikal A, Hess ST, Webb WW. Chem Phys. 2001; 274:37–55.
27. Liu Y, Kim HR, Heikal AA. J Phys Chem B. 2006; 110:24138–24146. [PubMed: 17125385]
28. Schwille P, Kummer S, Heikal AA, Moerner WE, Webb WW. Proc Natl Acad Sci USA. 2000; 97:151–156. [PubMed: 10618386]
29. Malvezzi-Campeggi F, Jahnz M, Heinze KG, Dittrich P, Schwille P. Biophys J. 2001; 81:1776–1785. [PubMed: 11509387]
30. Dickson RM, Cubitt AB, Tsien RY, Moerner WE. Nature. 1997; 388:355–358. [PubMed: 9237752]
31. Nagai T, Ibata K, Park ES, Kubota M, Mikoshiba K, Miyawaki A. Nat Biotechnol. 2002; 20:87–90. [PubMed: 11753368]
32. VanBeek DB, Zwier MC, Shorb JM, Krueger BP. Biophys J. 2007; 92:4168–4178. [PubMed: 17384068]
33. Kremers, GJ.; Goedhart, J. FRET and FLIM Techniques. Gadela, TWJ., editor. Vol. 334. Elsevier; 2009. p. 171-223.
34. Lam AJ. Nat Methods. 2012; 9:1005–1012. http://dx.doi.org/10.1038/nmeth.2171. [PubMed: 22961245]

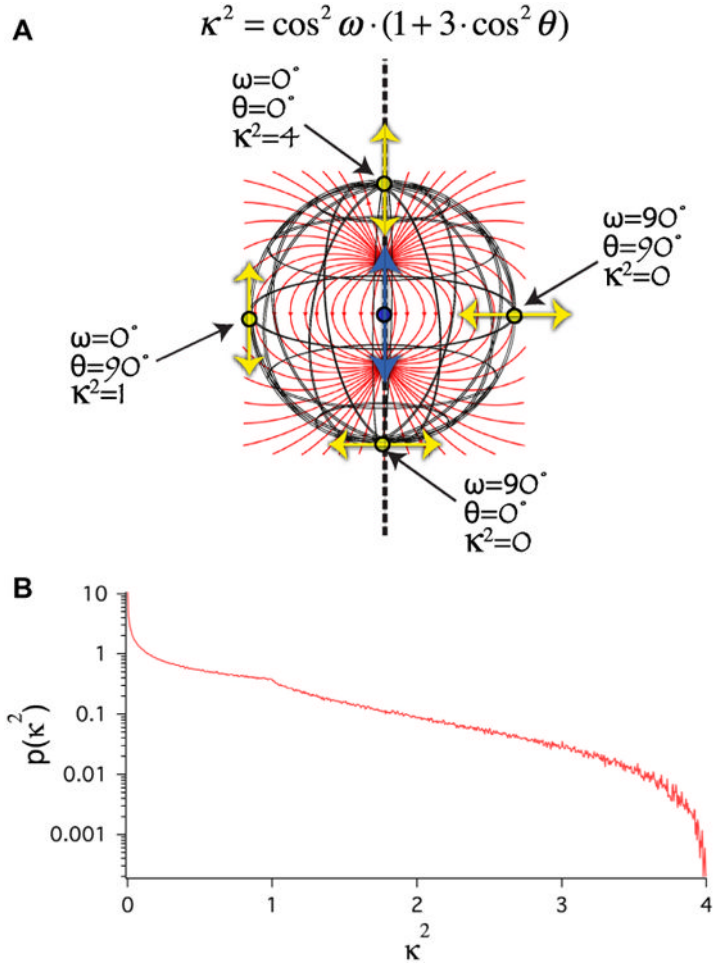

Fig. 1.

Isotropic κ^2 distribution. (A) Cartoon illustrating how the dipole orientation factor κ^2 is determined by 2 angles, θ and ω (see Eq. (5)). Blue arrow depicts the position and orientation of the donor emission dipole. Yellow arrows depict the position and orientation of four possible acceptor absorption dipoles, each the same distance from the donor. Red lines depict the local orientation of the electric field created by the excited state of the donor emission dipole. (B) Monte Carlo simulation of the κ^2 probability distribution assuming that θ and ω are randomly distributed (isotropic). Note that the mode of this distribution is 0 and the average is 2/3.

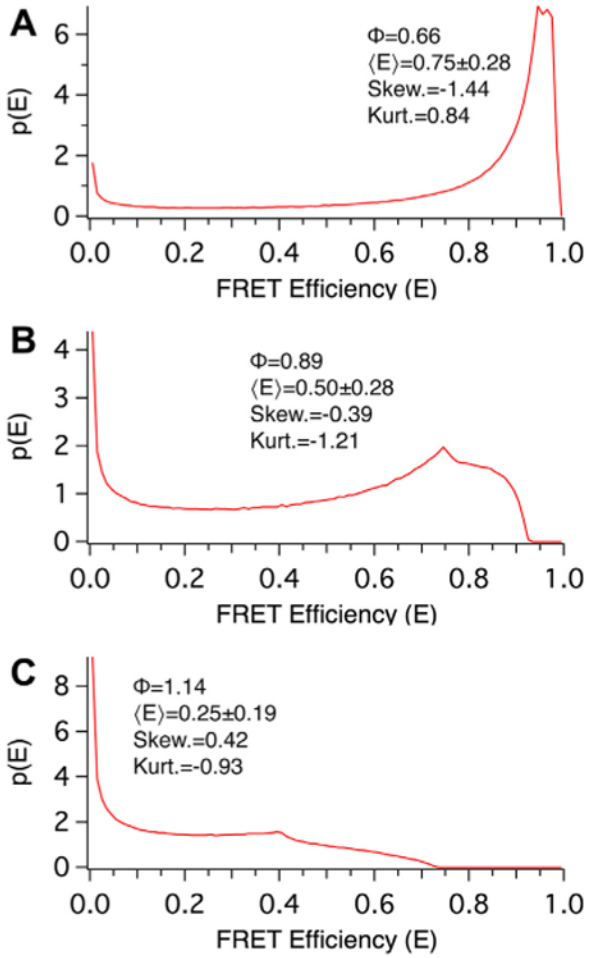

Fig. 2.

Monte Carlo simulations used to determine the relationship between average FRET efficiency and Separation under static isotropic conditions. The probability distribution of FRET efficiencies derived from Monte Carlo simulations where separation, normalized to the Förster distance (Φ), was set to values of 0.66 (A), 0.89 (B), and 1.14 (C), corresponding to average population FRET efficiencies, $\langle E \rangle$, of approximately 75%, 50%, and 25%, respectively. Note the irregular shapes of all three populations.

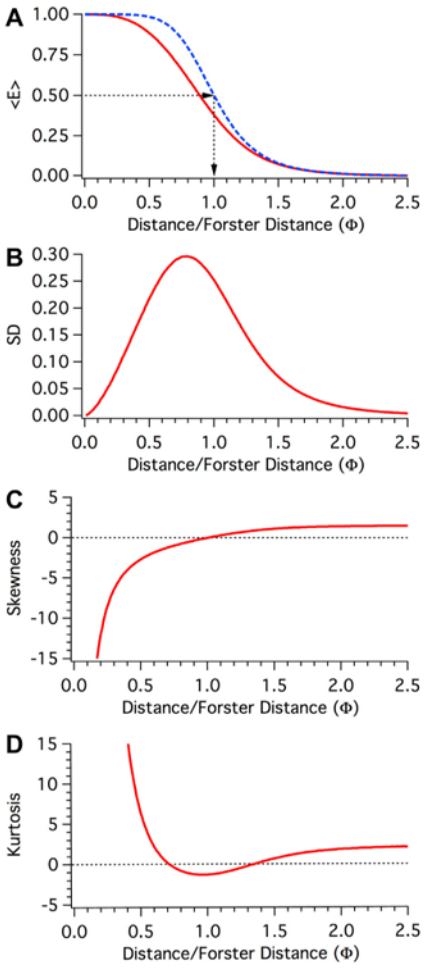

Fig. 3.

Moment Analysis of the dependence of FRET efficiency on Separation under static isotropic conditions. A. The dependence of $\langle E \rangle$ (the first moment of these populations) on Φ under isotropic dynamic (dashed Blue) or static (Red) conditions. (B) The dependence of variance (the second moment) on Φ under isotropic static conditions (Red). Plotted is the standard deviation of the distribution, which is the positive square root of the variance. (C) The dependence of skewness (the third moment) on Φ under isotropic static conditions (Red). The skewness represents symmetry within the distribution; a positive value indicates a heavier tail to the right, while a negative value indicates a left skewed distribution. (D). The dependence of kurtosis (the fourth moment) on Φ under isotropic static conditions (Red). The kurtosis represents the distribution peakedness relative to a normal distribution. A positive value indicates an acute peak in the distribution, while a negative value indicates a broad flat distribution.

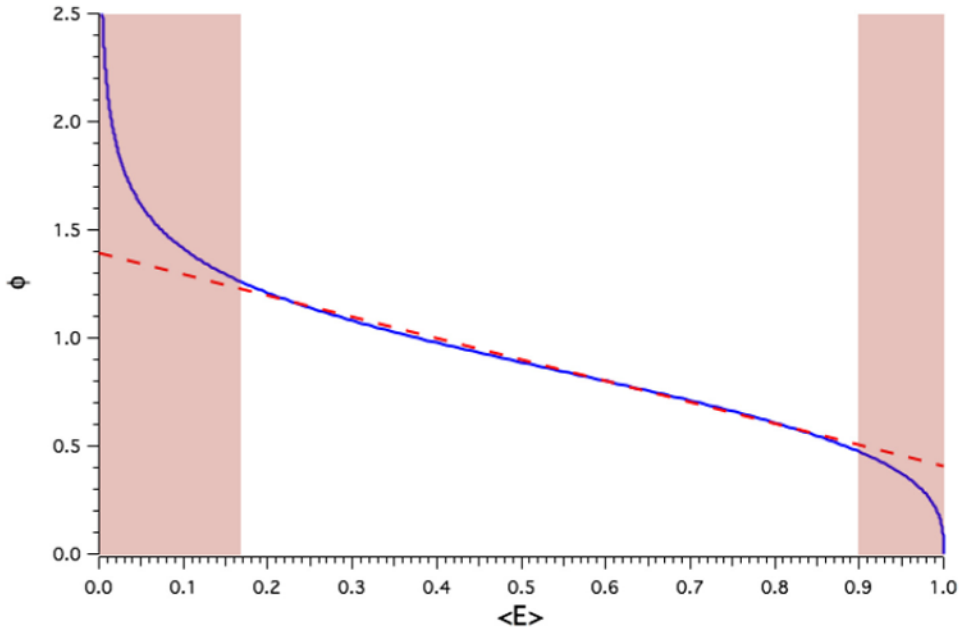

Fig. 4.

The dependence of Separation on average FRET efficiency under static isotropic conditions. The dependence of Φ on $\langle E \rangle$ under isotropic static (Blue) conditions. Dashed RED line depicts a linear fit to the central portion of the curve, while the RED tinted regions highlights average FRET efficiencies that correspond to the non-linear portions of the curve.

Table 1

The dependence of separation (Φ) on the average FRET efficiency (<E>) in the static isotropic regime.

<E>	Φ	<E>	Φ	<E>	Φ	<E>	Φ
0.999	0.01	**0.771**	0.64	**0.163**	1.27	**0.020**	1.90
0.999	0.02	**0.762**	0.65	**0.158**	1.28	**0.019**	1.91
0.999	0.03	**0.752**	0.66	**0.153**	1.29	**0.019**	1.92
0.999	0.04	**0.742**	0.67	**0.147**	1.30	**0.018**	1.93
0.999	0.05	**0.732**	0.68	**0.142**	1.31	**0.018**	1.94
0.999	0.06	**0.722**	0.69	**0.138**	1.32	**0.017**	1.95
0.999	0.07	**0.712**	0.7	**0.133**	1.33	**0.017**	1.96
0.999	0.08	**0.701**	0.71	**0.129**	1.34	**0.016**	1.97
0.999	0.09	**0.691**	0.72	**0.124**	1.35	**0.016**	1.98
0.999	0.10	**0.680**	0.73	**0.120**	1.36	**0.015**	1.99
0.998	0.11	**0.669**	0.74	**0.116**	1.37	**0.015**	2.00
0.998	0.12	**0.658**	0.75	**0.112**	1.38	**0.014**	2.01
0.997	0.13	**0.647**	0.76	**0.108**	1.39	**0.014**	2.02
0.997	0.14	**0.636**	0.77	**0.104**	1.40	**0.013**	2.03
0.996	0.15	**0.624**	0.78	**0.101**	1.41	**0.013**	2.04
0.996	0.16	**0.613**	0.79	**0.098**	1.42	**0.013**	2.05
0.995	0.17	**0.602**	0.80	**0.094**	1.43	**0.012**	2.06
0.994	0.18	**0.590**	0.81	**0.091**	1.44	**0.012**	2.07
0.993	0.19	**0.579**	0.82	**0.088**	1.45	**0.012**	2.08
0.992	0.20	**0.567**	0.83	**0.085**	1.46	**0.011**	2.09
0.991	0.21	**0.556**	0.84	**0.082**	1.47	**0.011**	2.10
0.989	0.22	**0.545**	0.85	**0.079**	1.48	**0.011**	2.11
0.988	0.23	**0.533**	0.86	**0.077**	1.49	**0.010**	2.12
0.986	0.24	**0.522**	0.87	**0.074**	1.50	**0.010**	2.13
0.984	0.25	**0.510**	0.88	**0.071**	1.51	**0.010**	2.14
0.982	0.26	**0.499**	0.89	**0.069**	1.52	**0.009**	2.15
0.980	0.27	**0.487**	0.90	**0.067**	1.53	**0.009**	2.16

<E>	Φ	<E>	Φ	<E>	Φ	<E>	Φ
0.978	0.28	**0.476**	0.91	**0.064**	1.54	**0.009**	2.17
0.976	0.29	**0.465**	0.92	**0.062**	1.55	**0.009**	2.18
0.973	0.30	**0.454**	0.93	**0.060**	1.56	**0.008**	2.19
0.971	0.31	**0.443**	0.94	**0.058**	1.57	**0.008**	2.20
0.968	0.32	**0.432**	0.95	**0.056**	1.58	**0.008**	2.21
0.965	0.33	**0.421**	0.96	**0.054**	1.59	**0.008**	2.22
0.962	0.34	**0.410**	0.97	**0.053**	1.60	**0.007**	2.23
0.958	0.35	**0.400**	0.98	**0.051**	1.61	**0.007**	2.24
0.955	0.36	**0.389**	0.99	**0.049**	1.62	**0.007**	2.25
0.951	0.37	**0.378**	1.00	**0.047**	1.63	**0.007**	2.26
0.947	0.38	**0.368**	1.01	**0.046**	1.64	**0.007**	2.27
0.943	0.39	**0.358**	1.02	**0.044**	1.65	**0.007**	2.28
0.939	0.40	**0.348**	1.03	**0.043**	1.66	**0.006**	2.29
0.934	0.41	**0.338**	1.04	**0.042**	1.67	**0.006**	2.30
0.929	0.42	**0.329**	1.05	**0.040**	1.68	**0.006**	2.31
0.925	0.43	**0.319**	1.06	**0.039**	1.69	**0.006**	2.32
0.919	0.44	**0.310**	1.07	**0.038**	1.70	**0.006**	2.33
0.914	0.45	**0.301**	1.08	**0.036**	1.71	**0.006**	2.34
0.908	0.46	**0.292**	1.09	**0.035**	1.72	**0.005**	2.35
0.903	0.47	**0.283**	1.10	**0.034**	1.73	**0.005**	2.36
0.897	0.48	**0.275**	1.11	**0.033**	1.74	**0.005**	2.37
0.890	0.49	**0.266**	1.12	**0.032**	1.75	**0.005**	2.38
0.884	0.50	**0.258**	1.13	**0.031**	1.76	**0.005**	2.39
0.877	0.51	**0.250**	1.14	**0.030**	1.77	**0.005**	2.40
0.870	0.52	**0.242**	1.15	**0.029**	1.78	**0.005**	2.41
0.863	0.53	**0.235**	1.16	**0.028**	1.79	**0.004**	2.42
0.856	0.54	**0.228**	1.17	**0.027**	1.80	**0.004**	2.43
0.848	0.55	**0.220**	1.18	**0.026**	1.81	**0.004**	2.44
0.841	0.56	**0.213**	1.19	**0.026**	1.82	**0.004**	2.45

<E>	Φ	<E>	Φ	<E>	Φ	<E>	Φ
0.833	0.57	**0.206**	1.20	**0.025**	1.83	**0.004**	2.46
0.825	0.58	**0.200**	1.21	**0.024**	1.84	**0.004**	2.47
0.816	0.59	**0.193**	1.22	**0.023**	1.85	**0.004**	2.48
0.808	0.60	**0.187**	1.23	**0.022**	1.86	**0.004**	2.49
0.799	0.61	**0.181**	1.24	**0.022**	1.87	**0.004**	2.50
0.790	0.62	**0.175**	1.25	**0.021**	1.88		
0.781	0.63	**0.169**	1.26	**0.020**	1.89		

Table 2

Förster distances (R0) for common fluorescent protein FRET pairs.

FP FRET-Pair	R_0	Refs.
ECFP-EYFP	4.7	*a*
ECFP-Citrine	4.8	*b*
mCerulean–mCherry	4.8	*a*
ECFP-Venus	5.0	*b*
mCerulean-EYFP	5.0	*a*
Cerulean–Venus	5.2	*b*
mCerulean–mVenus	5.3	*a*
SECFP-SEYFP	5.4	*b*
EGFP-mCherry	5.4	*b*
TagGFP-TagRFP	5.7	*b*
mTFP1-Citrine	5.7	*b*
mTFP1-mOrange	5.7	*b*
Citrine-mKate2	5.8	*b*
Clover-mCherry	5.8	*b*
mVenus-mCherry	5.8	*a*
mVenus-mOrange	5.8	*a*
mTurquoise1-SEYFP	5.8	*b*
mTurquoise2-SEYFP	5.9	*b*
Clover-mRuby2	6.3	*b*

[a] Kremers and Goedhart [33].

[b] Lam et al. [34].

Table 3

Estimating separation for fluorescent protein FRET standards.

Construct	<E>	→	Φ	×	R_0	=	$R_{DA\ Static}$	$R_{DA\ Dynamic}$	Ref.
C_5V	0.43		0.95		5.3		5.0	5.6	¶
$C_{17}V$	0.38		1.00		5.3		5.3	5.8	¶
$C_{32}V$	0.31		1.07		5.3		5.7	6.1	¶
$C_{40}V$	0.21		1.19		5.3		6.4	6.6	§
$C_{50}V$	0.13		1.34		5.3		7.1	7.3	§

¶Koushik et al. [21].

§Chen et al. [20].